

The target asymmetry in hard vector-meson electroproduction and parton angular momenta

S.V. Goloskokov ¹

*Bogoliubov Laboratory of Theoretical Physics, Joint Institute for Nuclear
Research,
Dubna 141980, Moscow region, Russia*

P. Kroll ²

*Fachbereich Physik, Universität Wuppertal, D-42097 Wuppertal, Germany
and
Institut für Theoretische Physik, Universität Regensburg,
D-93040 Regensburg, Germany*

Abstract

The target asymmetry for electroproduction of vector mesons is investigated within the handbag approach. While the generalized parton distribution (GPD) H is taken from a previous analysis of the electroproduction cross section, we here construct the GPD E from double distributions and constrain it by the Pauli form factors of the nucleon, positivity bounds and sum rules. Predictions for the target asymmetry are given for various vector mesons and discussed how experimental data on the asymmetry will further constrain E and what we may learn about the angular momenta the partons carry.

¹Email: goloskv@theor.jinr.ru

²Email: kroll@physik.uni-wuppertal.de

1 Introduction

The handbag approach to hard exclusive reactions which bases on factorization into hard subprocesses and soft GPDs, attracted the interest of many theoreticians and experimentalists in the last decade. The still poorly known GPDs as well as the quality and scantiness of the experimental data prevented definite conclusions about the applicability of the handbag approach in the experimentally accessible region of kinematics so far. Now, the situation is changing; we are in a stage where an increasing amount of precise data on hard exclusive reactions becomes available. The already accumulated data from JLAB, HERMES, COMPASS and HERA as well as those to be expected in the near future, will allow for an extraction of a wealth of qualitative and quantitative information on the GPDs. In a few years from now we will likely have accumulated sufficient information on the GPDs in order to answer the question in which range of kinematics the handbag approach can be applied to hard exclusive reactions in a consistent way.

Here in this work, we are going to investigate the target asymmetry A_{UT} for electroproduction of flavor neutral vector mesons (ρ^0 , ω , ϕ) and for the processes $ep \rightarrow e\rho^+n$ and $ep \rightarrow eK^{*0}\Sigma^+$. The asymmetry is related to the imaginary part of an interference term between the two GPDs H and E . Provided H is sufficiently well-known from an analysis of, say, the unpolarized cross section for electroproduction of vector mesons [1, 2], one may extract information on E from data on A_{UT} . Admittedly this is only possible in a model-dependent way, i.e. one unavoidably has to exploit an ansatz for E with a few free parameters which can be adjusted to experiment. Although the data on the target asymmetry will likely suffer from large experimental errors (cf. the recent, still preliminary HERMES result for ρ^0 production [3]) we believe and are going to substantiate this hope in the following, that the pattern of future A_{UT} data for various vector mesons will likely render such a determination of E feasible. Provided this program can be successfully carried through, one may evaluate Ji's sum rule [4] from H and E and learn about the angular momenta the partons inside the proton possess. The possibility of extracting information on the quark angular momenta from A_{UT} , at least for u and d quarks has been discussed by Ellinghaus *et al* [5] first. Here in this work, we will investigate improved parameterizations of the GPD E as compared to [5] and will also study the role of E for gluons and strange quarks.

In the next section we will briefly sketch the handbag formalism for the

processes of interest. In Sect. 3 we will present the model we use for the GPD E and discuss the constraints on its parameters. Predictions for A_{UT} are presented and discussed in Sect. 4. Concluding remarks will be presented in Sect. 5.

2 The handbag formalism

For the analysis of the target asymmetry for vector-meson (V) electroproduction we restrict ourselves to the kinematical region of small skewness ($\xi \lesssim 0.1$) and small invariant momentum transfer ($-t \lesssim 0.5 \text{ GeV}^2$) but large photon virtuality ($Q^2 \gtrsim 3 \text{ GeV}^2$) and large energy in the photon-proton center of mass frame ($W \gtrsim 5 \text{ GeV}$). In this kinematical region we have already investigated the $\gamma^*p \rightarrow Vp$ cross sections for unpolarized protons [1, 2, 6] and flavor neutral vector mesons and achieved very good agreement with the available data from HERMES, Fermilab and HERA. These cross sections are strongly dominated by contributions from the GPD H ; it is safe to neglect ³ the other GPDs E , \tilde{H} and \tilde{E} . In our previous work we calculated the quark ($\gamma^*q \rightarrow Vq$) and gluon ($\gamma^*g \rightarrow Vg$) subprocess amplitudes within the modified perturbative approach [7] in which quark transverse degrees of freedom as well as Sudakov suppressions are taken into account in the subprocess. This approach allows us to calculate not only the asymptotically dominant (longitudinal) amplitude for $\gamma_L^*p \rightarrow V_Lp$ but also the one for transversely polarized photons and vector mesons ($\gamma_T^*p \rightarrow V_Tp$). In contrast to the longitudinal amplitude the latter one cannot be calculated in collinear approximation since it suffers from infrared singularities in this limit [8, 9]. The quark transverse momenta, \mathbf{k}_\perp , provide an admittedly model-dependent regularization scheme of these singularities by replacements of the type

$$\frac{1}{dQ^2} \longrightarrow \frac{1}{dQ^2 + k_\perp^2} \quad (1)$$

in the parton propagators. Here, d is a momentum fraction or a product of two.

The dominant helicity amplitudes for the process $\gamma^*p \rightarrow VB$ are given

³We remark that in the unpolarized cross section there are no interference terms between H and the other GPDs up to corrections of order ξ^2 .

by

$$\begin{aligned}\mathcal{M}_{\mu+, \mu+}(V) &= \frac{e}{2} \left\{ \sum_a e_a \mathcal{C}_V^{aa} \langle H \rangle_{V\mu}^g + \sum_{ab} \mathcal{C}_V^{ab} \langle H \rangle_{V\mu}^{ab} \right\}, \\ \mathcal{M}_{\mu-, \mu+}(V) &= -\frac{e}{2} \frac{\sqrt{-t}}{M+m} \left\{ \sum_a e_a \mathcal{C}_V^{aa} \langle E \rangle_{V\mu}^g + \sum_{ab} \mathcal{C}_V^{ab} \langle E \rangle_{V\mu}^{ab} \right\},\end{aligned}\quad (2)$$

where some simplifications, relevant for the small ξ region, have been used. Thus, for instance, the contribution from E to the helicity non-flip amplitude, being proportional to ξ^2 , is neglected. The quark flavors are denoted by a, b while $e_{a(b)}$ denotes the quark charges in units of the positron charge e and m the proton mass. Besides the proton we consider also other ground state baryons, B , as for instance the Σ^+ (with mass M). With the help of flavor symmetry the $p \rightarrow B$ transition GPDs can be related to the proton ones [10]. The weight factors \mathcal{C}_V^{ab} comprise the flavor structure of the mesons. The non-zero weight factors for selected vector mesons read

$$\begin{aligned}\mathcal{C}_{\rho^0}^{uu} &= -\mathcal{C}_{\rho^0}^{dd} = \mathcal{C}_{\omega}^{uu} = \mathcal{C}_{\omega}^{dd} = 1/\sqrt{2}, & \mathcal{C}_{\phi}^{ss} &= 1, \\ \mathcal{C}_{\rho^+}^{ud} &= 1, & \mathcal{C}_{K^{*0}}^{ds} &= 1,\end{aligned}\quad (3)$$

The explicit helicities in (2) refer to the proton while μ is the helicity of the photon and the meson. Only the t dependence of the GPDs is taken into account in the amplitudes (2). That of the subprocess amplitudes \mathcal{H} provides corrections of order t/Q^2 which we neglect throughout this paper. In contrast to the subprocess amplitudes the t dependence of the GPDs is scaled by a soft parameter, actually by the slope of the diffraction peak. It can be shown [1] that in addition to the familiar parity-invariance relation the following symmetry relation

$$\mathcal{M}_{-\mu\nu', -\mu\nu} = \mathcal{M}_{\mu\nu', \mu\nu} \quad (4)$$

holds among the helicity amplitudes (2). Helicity flips in the $\gamma^* \rightarrow V$ transition have to be generated within the subprocess. Hence, amplitudes involving such helicity flips are suppressed by powers of $\sqrt{-t}/Q$ and consequently neglected.

The terms $\langle F \rangle$ denote convolutions of subprocess amplitudes and a GPD $F(= H, E)$. For the gluonic subprocess the convolutions read

$$\langle F \rangle_{V\mu}^g = \sum_{\lambda} \int_0^1 d\bar{x} \mathcal{H}_{\mu\lambda, \mu\lambda}^{Vg}(\bar{x}, \xi, Q^2, t=0) F^g(\bar{x}, \xi, t), \quad (5)$$

where the label λ refers to the helicities of the partons participating in the subprocess. The subprocess amplitudes \mathcal{H} are discussed in great detail in Ref. [1]. We refrain from repeating the lengthy expressions here. For the quark subprocesses we have

$$\langle F \rangle_{V\mu}^{ab} = \sum_{\lambda} \int_{-1}^1 d\bar{x} \mathcal{H}_{\mu\lambda, \mu\lambda}^{Vab}(\bar{x}, \xi, Q^2, t=0) F^{ab}(\bar{x}, \xi, t). \quad (6)$$

The quark GPDs for the proton and the $p \rightarrow n$ and $p \rightarrow \Sigma^+$ transitions are

$$F^{aa} = F^a, \quad F^{ab} = F^a - F^b \quad (a \neq b). \quad (7)$$

Since the resummation of the logarithms involved in the Sudakov factor can only be performed in the impact parameter space efficiently [7] we quote the subprocess amplitudes in that space

$$\begin{aligned} \mathcal{H}_{\mu\lambda, \mu\lambda}^{Vab} &= \int d\tau d^2b \hat{\Psi}_{V\mu}(\tau, -\mathbf{b}) \hat{\mathcal{F}}_{\mu\lambda, \mu\lambda}^{ab}(\bar{x}, \xi, \tau, Q^2, \mathbf{b}) \\ &\times \alpha_s(\mu_R) \exp[-S(\tau, \mathbf{b}, Q^2)]. \end{aligned} \quad (8)$$

For the Sudakov factor S , the choice of the renormalization (μ_R) and factorization (μ_F) scales as well as the hard scattering kernels $\hat{\mathcal{F}}$ or their respective Fourier transforms \mathcal{F} , we refer to Ref. [6]. In order to generalize to the case of flavored mesons the following replacements in quark propagators occurring in \mathcal{F} have to be made

$$T_s \longrightarrow e_a T_s, \quad T_u \longrightarrow e_b T_u. \quad (9)$$

The last item in (8) to be explained is $\hat{\Psi}_{V\mu}$, the Fourier transform of the momentum-space light-cone wave function for the vector meson. It is parameterized as a simple Gaussian ($j = L, T$)

$$\begin{aligned} \Psi_{Vj}(\tau, \mathbf{k}_{\perp}) &= 8\pi^2 \sqrt{2N_c} f_{Vj}(\mu_F) a_{Vj}^2 \left[1 + B_1^{Vj}(\mu_F) C_1^{3/2}(2\tau - 1) \right. \\ &\left. + B_2^{Vj}(\mu_F) C_2^{3/2}(2\tau - 1) \right] \exp[-a_{Vj}^2 \mathbf{k}_{\perp}^2 / (\tau\bar{\tau})]. \end{aligned} \quad (10)$$

The parameters of the ρ and ϕ wave functions are specified in [6]. The decay constants of longitudinally polarized ω and K^{*0} mesons are 187 and 218 MeV, respectively. For the ratio of f_{VT} and f_{VL} we take the QCD sum rule value of $\simeq 0.8$ at the scale of 1 GeV [11]. The Gegenbauer coefficients B_1^{Vj} are zero for all vector mesons except for the K^{*0} for which the values 0

and 0.1 are chosen. For the second Gegenbauer coefficients we take $B_2^{VL} = 0$ and $B_2^{VT} = 0.1$. All values of the Gegenbauer coefficients which are quoted at the scale 1 GeV, are in agreement with recent QCD sum rule analyses [11, 12], only B_2^{VL} is slightly smaller even with regard of the errors of the QCD sum rule results quoted in [11]. The evolution of the decay constants for transversely polarized vector mesons as well as that of the Gegenbauer coefficients with the factorization scale [13] is taken into account. Finally, for the transverse size parameters we take the values $a_{\omega j} = a_{K^*0j} = a_{\rho^+j} = a_{\rho^0j}$. The values of the latter parameters as well as those for the ϕ meson can be found in [6]. We note in passing that Gaussian wave functions of the type (10) are frequently used in phenomenology.

There is a minimal value of $-t$ allowed in the process of interest

$$t_{\min} = -\frac{2\xi}{1-\xi^2} [(1+\xi)M^2 - (1-\xi)m^2]. \quad (11)$$

Given the smallness of the $\Sigma^+ - p$ mass difference t_{\min} is small in all cases, practically of order ξ^2 and is therefore neglected as other effects of this order. We note that our helicities are light-cone ones which naturally occur in the handbag approach. The differences to the usual c.m.s. helicities are of order $m\sqrt{-t}/W^2$ [14] and can be ignored in the kinematical region of interest in this work. Skewness is related to Bjorken- x , x_{Bj} , by

$$\xi \simeq \frac{x_{Bj}}{2 - x_{Bj}} [1 + m_V^2/Q^2], \quad (12)$$

where m_V denotes the mass of the vector meson. The helicity amplitudes are normalized such that the partial cross sections for $\gamma_{L(T)}^* p \rightarrow V_{L(T)} p$ read (Λ is the usual Mandelstam function)

$$\frac{d\sigma_{L(T)}}{dt} = \frac{1}{16\pi(W^2 - m^2)\sqrt{\Lambda(W^2, -Q^2, m^2)}} \sum_{\nu'} |\mathcal{M}_{0(+)\nu', 0(+)+}|^2, \quad (13)$$

which holds with regard to the above-mentioned simplifications. For most of the processes of interest the proton helicity flip amplitude can be neglected in (13); the only exception is the ρ^+ channel. The cross sections, integrated upon t , are denoted by σ_L and σ_T . The full (un-separated) cross section for $\gamma^* p \rightarrow V p$ is

$$\sigma = \sigma_T + \varepsilon\sigma_L, \quad (14)$$

in which ε is the familiar ratio of longitudinal to transverse photon fluxes. The power corrections of kinematical origin included in Eq. (12) and in the phase space factor (13) are taken into account by us. With the exception of these kinematical effects hadron masses are omitted otherwise.

Following the conventions specified in [15] (see also [16]) the target asymmetry for $\gamma^*p \rightarrow VB$ reads

$$A_{UT} = -2 \frac{\text{Im}[\mathcal{M}_{+-,++}^* \mathcal{M}_{++,++}] + \varepsilon \text{Im}[\mathcal{M}_{0-,0+}^* \mathcal{M}_{0+,0+}]}{\sum_{\nu'} [|\mathcal{M}_{+\nu',++}|^2 + \varepsilon |\mathcal{M}_{0\nu',0+}|^2]}. \quad (15)$$

It is measured as the $\sin(\phi - \phi_S)$ moment of the cross section for electroproduction of vector meson with a transversally polarized proton target where ϕ is the azimuthal angle between the lepton and hadron plane and ϕ_S the azimuthal angle of the target spin vector defined with respect to the lepton plane [15].

3 Modeling E

3.1 Valence quarks

Not much is known about E as yet. Some information on it comes from the zero-skewness analysis [17] of the Pauli form factor of the nucleon. This electromagnetic form factor is odd under charge conjugation and therefore only sensitive to valence quarks ($q_{\text{val}} = q - \bar{q}$). The forward limit $t = \xi = 0$ of E_{val} is parameterized like that of H , i.e. the familiar parton distribution functions (PDFs),

$$\begin{aligned} e_{\text{val}}^a(x) &= E_{\text{val}}^a(x, \xi = 0, t = 0) \\ &= \frac{\Gamma(2 - \alpha_{\text{val}} + \beta_{\text{val}}^a)}{\Gamma(1 - \alpha_{\text{val}})\Gamma(1 + \beta_{\text{val}}^a)} \kappa_a x^{-\alpha_{\text{val}}(0)} (1 - x)^{\beta_{\text{val}}^a}. \end{aligned} \quad (16)$$

The moments of e_{val}^a read ⁴

$$e_{n0}^{av} = \int_0^1 dx x^{n-1} e_{\text{val}}^a(x) = \kappa_a \frac{\Gamma(2 - \alpha_{\text{val}} + \beta_{\text{val}}^a)}{\Gamma(1 + n - \alpha_{\text{val}} + \beta_{\text{val}}^a)} \frac{\Gamma(n - \alpha_{\text{val}})}{\Gamma(1 - \alpha_{\text{val}})}. \quad (17)$$

⁴Generally the forward limit of a GPD F is defined as $f^a(x) = F^a(x, \xi = 0, t = 0)$ for quarks and $xf^g(x) = F^g(x, \xi = 0, t = 0)$ for gluons ($x \geq 0$). The n -th moment of f^i ($i = a, g$) is defined as $f_{n0}^i = \int_0^1 dx x^{n-1} f^i(x)$. This definition holds for antiquarks too.

As can be seen from this expression the pre-factor in (16) ensures the normalization

$$e_{10}^{a_v} = \kappa_a, \quad (18)$$

where κ_a is the contribution of flavor- a quarks to the anomalous magnetic moment of the proton ($\kappa_u \simeq 1.67$, $\kappa_d \simeq -2.03$). The forward limit (16) of E can be used as input to the familiar double distribution ansatz [18]

$$f_{\text{val}}^a(\beta, \alpha, t) = e^{b_{\text{val}}^e t} \beta^{-\alpha'_{\text{val}} t} e_{\text{val}}^a(\beta) \frac{3}{4} \frac{[(1-\beta)^2 - \alpha^2]}{(1-\beta)^3} \Theta(\beta). \quad (19)$$

The GPD is subsequently obtained from the integral

$$E_{\text{val}}^a(\bar{x}, \xi, t) = \int_{-1}^1 d\beta \int_{-1+|\beta|}^{1-|\beta|} d\alpha \delta(\beta + \xi\alpha - \bar{x}) f_{\text{val}}^a(\beta, \alpha, t). \quad (20)$$

The t dependence in (19) is a small- t simplification of the more complicated profile function used in [17]. $\alpha_{\text{val}}(t) = \alpha_{\text{val}}(0) + \alpha'_{\text{val}} t$ is a standard Regge trajectory for which we take the numerical values $\alpha_{\text{val}}(0) = 0.48$ and $\alpha'_{\text{val}} = 0.9 \text{ GeV}^{-2}$ and b_{val}^e is a parameter that describes the t dependence of the Regge residue. In accord with [6] we take $b_{\text{val}}^e = 0$. Possible dependencies of the Regge trajectory and b_{val}^e on the quark flavor is ignored by us. In the form factor analysis performed in [17] for instance a value of 0.38 GeV^{-2} for b_{val}^e has been found for u -valence and -0.75 GeV^{-2} for d -valence quarks. Our value may be viewed as a rough average of these values.

In Ref. [17] the powers β_{val}^a have been determined. The best fit values which hold at a scale of $Q_0 = 2 \text{ GeV}$, are

$$\beta_{\text{val}}^u = 4, \quad \beta_{\text{val}}^d = 5.6. \quad (21)$$

However, β_{val}^u can be varied between 4 and 6, β_{val}^d between 5 and 6 and still reasonable fits of the Pauli form factors are achieved ⁵. These parameter regions are taken into account in our error assessment to be discussed below. Fits with β_{val}^u substantially larger than β_{val}^d lead to results of lesser, just tolerable quality.

⁵The analysis of the Pauli form factor suffers from the large number of free parameters. In contrast to the analysis of the Dirac form factor the forward limit e_{val}^a has to be determined as well. Hence, not all parameters can be freed in the fits to the Pauli form factors.

There is a remarkable feature of the parameterization (16). With the help of (17) one can write the ratio of sum and difference of the second moments as

$$\frac{e_{20}^{u_v} + e_{20}^{d_v}}{e_{20}^{u_v} - e_{20}^{d_v}} = \frac{\kappa_u + \kappa_d}{\kappa_u - \kappa_d} \frac{1 + \frac{\kappa_u}{\kappa_u + \kappa_d} \frac{\beta_{\text{val}}^d - \beta_{\text{val}}^u}{2 - \alpha_{\text{val}} + \beta_{\text{val}}^u}}{1 + \frac{\kappa_u}{\kappa_u - \kappa_d} \frac{\beta_{\text{val}}^d - \beta_{\text{val}}^u}{2 - \alpha_{\text{val}} + \beta_{\text{val}}^u}}. \quad (22)$$

This expression tells us that for $\beta_{\text{val}}^d > \beta_{\text{val}}^u$ this combination of moments is smaller than the corresponding ratio of the first moments

$$\frac{\kappa_u + \kappa_d}{\kappa_u - \kappa_d} = -0.097. \quad (23)$$

On the other hand, for $\beta_{\text{val}}^u > \beta_{\text{val}}^d$ (22) is larger than (23). Note that in the chiral soliton model one finds $e_{20}^{u_v} + e_{20}^{d_v} = 0$ in the large- N_c limit [19]. In the limit of an infinitely large factorization scale QCD predicts $\sum_a e_{20}^a = 0$ as Ji showed [20]. These two results support to some extent the findings of Ref. [17] that the Pauli form factor favors $\beta_{\text{val}}^d \geq \beta_{\text{val}}^u$. Finally we remark that E_{val}^a constructed from e_{val}^a through the double distribution ansatz (19), (20), respects the inequalities which ensure the positivity of the quark densities for various combinations of proton and quark spins [17, 21, 22].

3.2 Gluons and sea quarks

In order to model E for gluons and sea quarks we follow Diehl and Kugler [16] and have recourse to positivity bounds and to a sum rule that follows from a combination of Ji's sum rule [4] and the momentum sum rule known from deep inelastic lepton-nucleon scattering

$$e_{20}^g = - \sum_a e_{20}^{a_v} - 2 \sum_a e_{20}^{\bar{a}}. \quad (24)$$

For obvious reasons we split the quark GPDs into valence and sea quark contributions (using $E^{\bar{q}}(x, \xi, t) = -E^q(-x, \xi, t)$). As we discussed in the Sect. 3.1 the analysis of the Pauli form factor favors a very small value of the valence quark term in (24). Thus, the gluon and sea quark moments have to cancel each other almost completely. Assuming in analogy to the situation for H , small sea quark contributions, we have to conclude from these considerations that the gluon moment at $t = 0$ is very small, in fact smaller than the individual valence quark moments. Another argument that points

into the same direction comes from the Regge behaviour of E^g . As is well-known the familiar soft Pomeron exchange dominantly couples to the proton helicity non-flip vertex while its flip coupling is very small. In fact, it is hard to find convincing evidence for a non-zero flip coupling phenomenologically [23]. Supposing that this behavior also holds for the hard gluonic Regge exchange controlling H^g and E^g at low- x , we are forced to infer that $E^g \simeq 0$. Thus, the relative importance of gluon and valence quark GPDs are likely very different for E and H for which H^g is large. On account of this one may neglect E for gluons and sea quarks in a first attempt and estimate A_{UT} and spin density matrix elements (SDMEs) for a transversely polarized proton target just from E_{val}^a .

In order to elucidate the role of E^g and E^{sea} in more detail we also study scenarios for which these GPDs are non-zero. Again we employ the double distribution ansatz for them ⁶. The corresponding forward limits are parameterized in analogy to (16)

$$\begin{aligned} e^s &= N_s x^{-1-\delta} (1-x)^{\beta^s}, \\ e^g &= N_g x^{-1-\delta} (1-x)^{\beta^g}, \end{aligned} \quad (25)$$

For simplicity a flavor symmetric sea is assumed. The low- x behavior of both these GPDs is assumed to be controlled by the gluon trajectory for which we use $\delta = 0.1 + 0.06 \ln(Q^2/Q_0^2)$ and $\alpha'_g = 0.15 \text{ GeV}^{-2}$ for its slope. The gluon trajectory has been fixed in our analysis of the cross sections for ρ^0 and ϕ electroproduction [2, 6].

Further help in fixing the gluon and sea quark GPD comes from the positivity bounds. For an exponential t dependence of the corresponding double distributions with profile functions $g_i(x)$ for E^i and $f_i(x)$ for H^i [2, 6] (cf. (19))

$$\begin{aligned} g_s &= g_g = \alpha'_g \ln 1/x + b_g^e, \\ f_s &= f_g = \alpha'_g \ln 1/x + b_g, \end{aligned} \quad (26)$$

one finds the following bounds [17]

$$\begin{aligned} \left[\frac{e_s(x)}{s(x)} \right]^2 &\leq 21.75 m^2 \left[\frac{g_s(x)}{f_s(x)} \right]^3 [f_s(x) - g_s(x)], \\ \left[\frac{e_g(x)}{g(x)} \right]^2 &\leq 21.75 m^2 \left[\frac{g_g(x)}{f_g(x)} \right]^3 [f_g(x) - g_g(x)]. \end{aligned} \quad (27)$$

⁶Possible D terms [24] in E are identical to those occurring in H where we have neglected them [1, 2] and, therefore, in E too.

These bounds ensure positive semi-definite densities of partons in the transverse plane [22]. Contributions from the polarized PDFs are neglected in (27) which appears reasonable for not too large values of x since there is growing experimental evidence that Δg and Δs are very small in that region of x , see for instance [25, 26]. Inserting the profile functions (26) into the bounds (27), we find ($i = s, g$)

$$\beta^i \geq 6, \quad b_g^e < b_g. \quad (28)$$

The present data do not provide any other information on b_g^e . We therefore follow [16] and assume $b_g^e = 0.9b_g$. The parameter b_g is taken from our previous work [2, 6]. It has the value

$$b_g = 2.58 \text{ GeV}^{-2} + 0.25 \text{ GeV}^{-2} \ln [m^2/(Q^2 + m^2)]. \quad (29)$$

The restriction of β^i guarantees the dominance of the valence quarks at large x .

We investigate the following variants of E (see Tab. 1): Besides our default case, the variant 1, with the powers (21) and $E^g \simeq E^s \simeq 0$ we try three more examples: For variant 2 (with $N_s > 0$) and 3 (with $N_s < 0$) we choose $\beta^s = 7$ and $|N^s|$ as large as the bound (27) allows. In fact its saturation occurs at $x \simeq 0.1$. For these variants we choose $\beta^g = 6$ and fix N_g by (24). Variant 4 is an extreme case for which we assume a large value of β_{val}^u and a small value of β_{val}^d . For this choice the Pauli form factor of the proton is still fitted although with a low quality ⁷. The valence quarks now contribute substantially to the sum rule (24). We assume $E^s = 0$ for this variant, take $\beta^g = 7$ and fix N_g by (24) again. One may also consider a variant where E for the valence quarks is the same as for variant 4 but trying to saturate the sum rule (24) solely by the sea quarks. However, this would require a very large sea-quark GPD which violates the positivity bound (27). Finally we investigate the case $\beta_{\text{val}}^u = \beta_{\text{val}}^d = 6$ and saturate the sum rule (24) either by the gluon (variant 5) or by the sea quarks (variant 6). In Tab. 1 the parameters of the six variants are compiled. It is to be emphasized that for all variants we consider the gluonic GPD E^g is far below the bound (27) since the gluon PDF $g(x)$ is very large.

⁷The JLab measurement E02-13 of the electric form factor of the neutron for Q^2 up to 3.5 GeV^2 will tell us whether or not the choice $\beta_{\text{val}}^u > \beta_{\text{val}}^d$ is realistic. The data are not yet available.

var.	β_{val}^u	β_{val}^d	β^g	β^s	N_g	N_s	J^u	J^d	J^s	J^g
1	4	5.6	-	-	0.000	0.000	0.250	0.020	0.015	0.214
2	4	5.6	6	7	-0.873	0.155	0.276	0.046	0.041	0.132
3	4	5.6	6	7	0.776	-0.155	0.225	-0.005	-0.011	0.286
4	10	5	7	-	0.523	0.000	0.209	0.013	0.015	0.257
5	6	6	7	-	0.167	0.000	0.230	0.024	0.015	0.228
6	6	6	-	7	0.000	0.025	0.234	0.028	0.019	0.214

Table 1: The parameters of the forward limits of the GPD E and the angular momentum the various partons carry. $\alpha = 0.48$ throughout. The parameters and the angular momenta are quoted at a scale of 2 GeV.

3.3 Parton angular momenta

In Tab. 1 we also quote the angular momenta of the quarks and the gluons evaluated from Ji's sum rule [4]

$$\begin{aligned}
\langle J^a \rangle &= \frac{1}{2} [e_{20}^{a_v} + h_{20}^{a_v}] + e_{20}^{\bar{a}} + h_{20}^{\bar{a}}, \\
\langle J^g \rangle &= \frac{1}{2} [e_{20}^g + h_{20}^g].
\end{aligned} \tag{30}$$

The second moments of H at $\xi = t = 0$ are evaluated from the CTEQ6 PDFs [27]. The following values have been obtained:

$$\begin{aligned}
h_{20}^{u_v} &= 0.288, & h_{20}^{d_v} &= 0.118, & h_{20}^g &= 0.428, \\
h_{20}^{\bar{u}} &= 0.028, & h_{20}^{\bar{d}} &= 0.035, & h_{20}^s &= 0.015,
\end{aligned} \tag{31}$$

at a scale of 2 GeV. Note that $\langle J^a \rangle$ is the average three-component of the angular momentum quarks of flavor a and their antiquarks carry. The angular momenta of the various partons do not sum exactly to 1/2, the spin of the proton, since the moments quoted in (31) do not exactly saturate the momentum sum rule of deep inelastic lepton-nucleon scattering (actually $\sum_i h_{20}^i = 0.990$) because of the neglected charm distribution. The values

quoted in Tab. 1 reveal a characteristic pattern: for all the variants we investigate the angular momenta of the u quarks and the gluon are large while those of the d and s quarks are small. Hence, the spin of the proton is essentially made up by the angular momenta of the u quarks and the gluons. In Ref. [17] further solutions for E_{val}^u and E_{val}^d are given which are also compatible with the data on the Pauli form factor of the proton. These solutions, completed if necessary by E^g and/or E^s in the same fashion as we constructed the variants quoted in Tab. 1, provide results for the angular momenta which lie between the extreme values of the variants shown in the table. The present theoretical uncertainties of the angular momenta are indicated by the spread of the values for J^i quoted in Tab. 1.

The angular momenta of the valence quarks are

$$\langle J^{u_v} \rangle = 0.222, \quad \langle J^{d_v} \rangle = -0.015, \quad (32)$$

for the variants 1,2 and 3. Slightly different values are obtained for the other variants. These values agree well with those derived in [17] within the errors estimated in the latter work. The largest deviation occurs for variant 4 for which the angular momenta of the valence quarks are about 1.5 standard deviations smaller than the results found in [17] ($\langle J^{u_v} \rangle = 0.211(17)$, $\langle J^{d_v} \rangle = 0.000(19)$). In Ref. [28] the angular momenta of u and d quarks have been calculated from lattice QCD using domain wall valence quarks and improved staggered sea quarks in heavy quark scenarios. After extrapolation to the physical value of the pion mass they obtain

$$\langle J^u \rangle = 0.214(27), \quad \langle J^d \rangle = -0.001(27). \quad (33)$$

It should be stressed that these results are rather to be interpreted as the angular momenta of the valence quarks although after the extrapolation they may contain sea quark effects. Obviously, our values for the valence quarks agree with the lattice results. The angular momenta of the gluons have been estimated using QCD sum rules [29] and a quark model [30]. The values found ($\langle J^g \rangle \simeq 0.25$ [29] and $\simeq 0.24$ [30] at the respective low scales of 1 and 0.5 GeV, lie within the range of results quoted in Tab. 1 even though on the side of larger values.

The orbital angular momentum of the partons may be obtained from (30) by subtracting the corresponding first moments of \tilde{H} . In Ref. [31] (scenario 1, NLO) the moments of the polarized valence quarks PDFs are evaluated to

$$\tilde{h}_{10}^{u_v} = 0.926, \quad \tilde{h}_{10}^{d_v} = -0.341, \quad (34)$$

at the scale of 2 GeV. Just for orientation we quote the values of the orbital angular momenta of the valence quarks for variants 1,2 and 3 at our default scale

$$\langle L^{uv} \rangle \simeq -0.241, \quad \langle L^{dv} \rangle \simeq 0.155. \quad (35)$$

In the analysis of Ref. [31] the first moment of the polarized gluon distribution, $x\Delta g(x)$, is subject to huge errors and cannot be used here. Because of the smallness of $x\Delta g(x)$ at least for small x [25, 26] we expect $\tilde{h}_{10}^g \simeq 0$ and, hence, $\langle L^g \rangle \simeq \langle J^g \rangle$. We note in passing that in a recent analysis of the polarized PDFs [32] a gluon moment \tilde{h}_{10}^g has been found that is compatible with zero at least at the scale of 3.16 GeV.

4 Discussion of the results on A_{UT}

Having specified various variants of the GPD E and taking H from [2] we are in the position to evaluate A_{UT} for electroproduction of various vector mesons. Of course we also obtain results for the cross sections (separated and unseparated). In [2, 6] we have already compared the predictions for the cross sections with experiment in great detail for the cases of ρ^0 and ϕ production and found generally excellent agreement with the data from HERMES, HERA and FNAL in a large range of kinematics. Predictions for the unseparated integrated cross sections for ω , ρ^+ and K^{*0} electroproduction are shown in Fig. 1 where, for comparison, also results for ρ^0 production are displayed. The theoretical uncertainties of our results for the cross sections are estimated from the Hessian errors of the CTEQ6 PDFs, cf. the discussion in [2, 6]. Due to neglected power corrections of order m^2/Q^2 and $-t/Q^2$ and the possibility of large higher order perturbative QCD corrections [16, 33] we do not provide results for $Q^2 < 3 \text{ GeV}^2$.

The cross sections for ρ^0 , ϕ and ω production increase with energy at fixed Q^2 due to considerable contributions from the gluonic subprocess $\gamma^*g \rightarrow Vg$ which grow $\propto W^{4\delta(Q^2)}$ for $\xi \rightarrow 0$. This behaviour is to be contrasted with the cross sections for $\gamma^*p \rightarrow K^{*0}\Sigma^+$ and $\gamma^*p \rightarrow \rho^+p$ to which the gluons do not contribute. These cross sections are predicted to shrink with energy since the dominant valence quark contributions lead to $\sigma \propto W^{4(\alpha_{\text{val}}(0)-1)}$ for $\xi \rightarrow 0$. The shrinkage is milder for K^{*0} than for the ρ^+ channel due to the strange quark contribution which has the same energy dependence as the gluon one. Lack of data for these two processes prevent the verification of our results as yet. It would be very interesting to learn whether the adopted

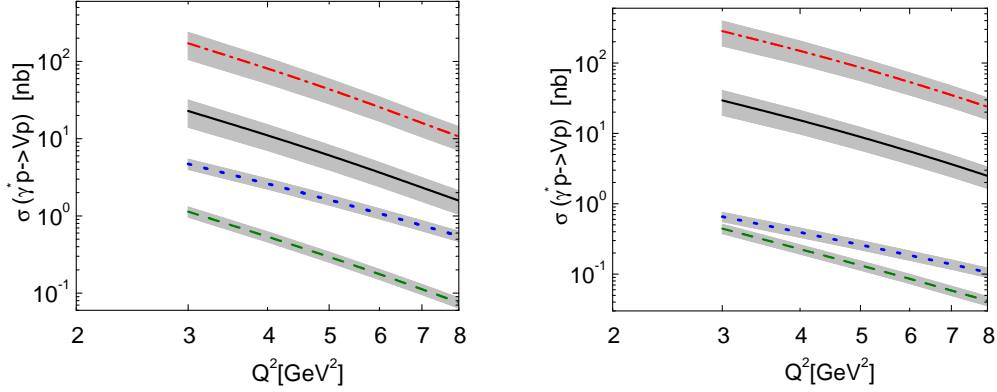


Figure 1: The integrated cross section for vector-meson electroproduction at $W = 5$ (left) and 10 GeV (right). The solid (dashed, dotted, dash-dotted) line represents the results evaluated from variant 1 for ω (K^{*0} , ρ^+ , ρ^0) production. The shaded bands indicate the theoretical uncertainties of our predictions. For the K^{*0} wave functions the Gegenbauer coefficients $B_1^{K^{*0}L(T)}$ are taken to be zero.

Q^2 -independent intercept of the valence quark Regge trajectory is indeed required by experiment.

In Fig. 2 we show the predictions for A_{UT} for ρ^0 production at $W = 5$ GeV integrated upon $0 \leq -t \leq 0.5$ GeV² ($t \simeq t'$ at small skewness) and versus t at $Q^2 = 3$ GeV². The uncertainties of our results follow from those of the CTEQ6 PDFs and the parametric errors of the GPD E . Note that the variants 2 and 3 are very similar to the default variant 1, i.e. the sea and gluon contributions cancel each other to a large extent. The results obtained with variants 5 and 6 also lie within the error bands but are not shown here and in the following for better legibility of the figures. Only variant 4 exhibits a distinctively different behaviour - A_{UT} is now positive. Our predictions obtained from the various variants agree with preliminary data from HERMES [3]. Even variant 4 is not ruled out given the experimental and theoretical errors. HERMES also provides A_{UT} separately for longitudinally and transversally polarized photons: $A_{UT}(\rho_L^0) = 0.04 \pm 0.12$ and $A_{UT}(\rho_T^0) = -0.08 \pm 0.10$ at $W = 5$ GeV and $Q^2 = 3.07$ GeV². We find $A_{UT}(\rho_L^0) \simeq A_{UT}(\rho_T^0) = -0.020$ for the default variant. Although there is agreement within errors we stress that the same sign is obtained for both these observables. The origin of this fact can be traced back to the smallness of the phases between the transverse

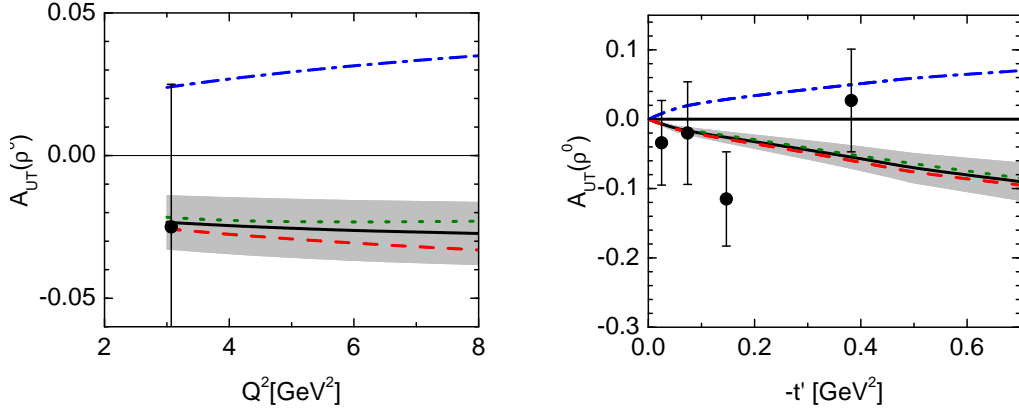


Figure 2: The asymmetry A_{UT} for ρ^0 production versus Q^2 , integrated upon t , (left) and versus t' at $Q^2 = 3 \text{ GeV}^2$ (right) at an energy of 5 GeV. The solid (dashed, dotted, dash-dotted) line represents the results for variant 1 (2, 3, 4). The shaded band indicates the theoretical uncertainty of the predictions for variant 1. The other variants have similar uncertainties. Preliminary data are taken from HERMES [3], the t dependent ones are at $Q^2 = 2 \text{ GeV}^2$.

and longitudinal amplitudes, about 3 degrees, for both proton helicity flip and non-flip. Consequences of this feature of our handbag approach for the spin density matrix elements of the ρ^0 meson have been discussed in [6]. In trend the predicted t dependence is in agreement with the preliminary HERMES data [3] which are measured at the admittedly low value ⁸ of 2 GeV² for Q^2 .

The target asymmetry for ω and ρ^+ production at the same energy is shown in Fig. 3. For ω production A_{UT} behaves similar to that for ρ^0 production except that it is about a factor of 5 larger in absolute value. This comes about from the flavor weight factors (3) for the dominant valence quark contributions

$$\mathcal{M}_{\mu-, \mu+}(\rho^0) \sim \langle e_u E_{\text{val}}^u - e_d E_{\text{val}}^d \rangle \quad \mathcal{M}_{\mu-, \mu+}(\omega) \sim \langle e_u E_{\text{val}}^u + e_d E_{\text{val}}^d \rangle. \quad (36)$$

With $E_{\text{val}}^u \simeq -E_{\text{val}}^d$ as is indicated by the anomalous magnetic moments of the

⁸We stress that in principle A_{UT} can also be calculated at Q^2 lower than say 3 GeV². The trends of A_{UT} to be seen from the figures, simply propagate down to smaller Q^2 . What prevents us from doing so is the fact that the theoretical uncertainties of the predictions are not under control at low Q^2 because of the neglected power and higher order QCD corrections.

quarks, κ_a , which fix the normalization of E_{val}^a , and corresponding effects in the non-flip amplitudes the enhancement of $A_{UT}(\omega)$ over $A_{UT}(\rho^0)$ in absolute value is evident.

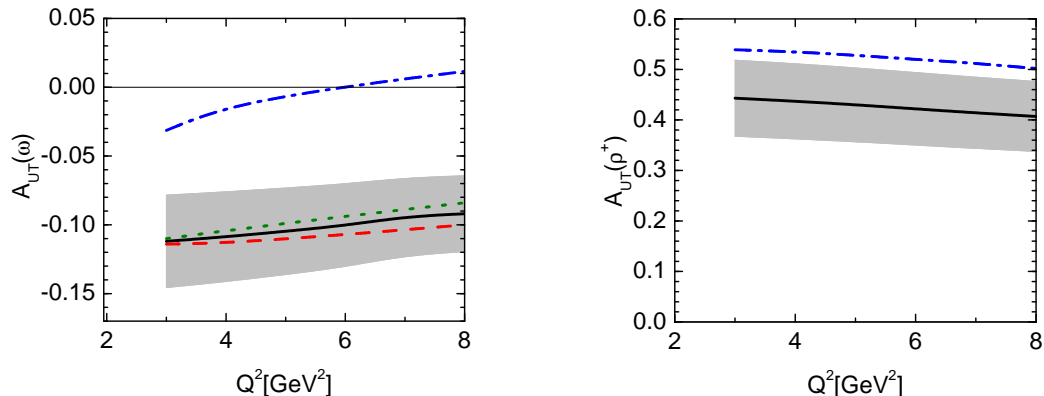


Figure 3: As in Fig. 2 but for ω (left) and ρ^+ production (right).

For ρ^+ production only u and d quark GPDs contribute. In fact they occur in the combination

$$F^u - F^d \simeq F_{\text{val}}^u - F_{\text{val}}^d \quad (37)$$

where F is either H or E . The sea quark contributions cancel to a large extent in the difference at small ξ (cf. the discussion in [2]). Therefore the variants 1, 2 and 3 fall together for this channel. Since $0 < H_{\text{val}}^d < H_{\text{val}}^u$ and $E_{\text{val}}^u \simeq -E_{\text{val}}^d$ it is evident that the proton helicity-flip amplitude is large in this case and leads to a very large $A_{UT}(\rho^+)$, see Fig. 3.

Another interesting case is K^{*0} production. Neither the gluonic GPDs contribute nor those for u quarks; only the difference $F^d - F^s$ occurs. As a consequence the cross section is very small. On the other hand, A_{UT} is rather large in absolute value. This can be seen from Fig. 4 where we also display results obtained from variant 1 but using the value 0.1 for the first Gegenbauer coefficient, $B_1^{K^{*0}L(T)}$, of the K^{*0} wave function instead of zero as employed for the other cases. The dependence on the Gegenbauer coefficient is mild. Since the sea in E is assumed to be flavor symmetric the results for variants 1, 2 and 3 fall together.

We do not display results for ϕ production. They are tiny, typically less than 0.005 in absolute value and for the default variant even zero. The theoretical uncertainties of our predictions for $A_{UT}(\phi)$ are estimated to amount to

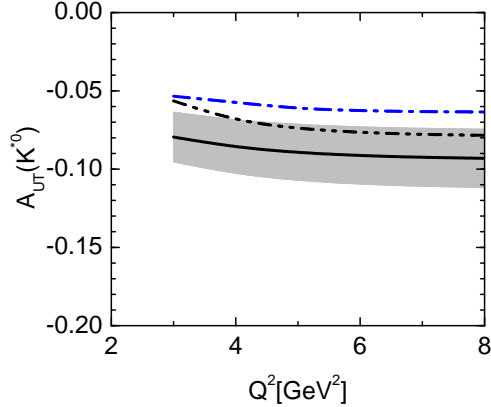


Figure 4: The target asymmetry for K^{*0} production at $W = 5$ GeV. The solid (dash-dotted) line represents our results for variant 1 (4) using $B_1^{K^{*0}L(T)} = 0$. The dot-dot-dashed line are the results evaluated from variant 1 with $B_1^{K^{*0}L(T)} = 0.1$.

about 0.01. The small values of $A_{UT}(\phi)$ is not a surprise given the smallness of the contributions from E^g and E^s and their partial cancellations for variants 2 and 3. A preliminary HERMES result [34] of $A_{UT}(\phi) = -0.05 \pm 0.12$ at $W \simeq 4.5$ GeV and $Q^2 = 1.9$ GeV² is compatible with our results in trend although the experimental error is too large for permitting any conclusion. The preliminary HERMES results [34] on $A_{UT}(\phi)$ for either longitudinally or transversally polarized photons are also compatible with zero within large errors.

The t dependence of A_{UT} for the processes of interest, evaluated from variant 1 at $W = 5$ GeV and $Q^2 = 3$ GeV² is shown in Fig. 5. While for ω and K^{*0} production it is similar to that of the ρ^0 case (see Fig. 2) it is quite different for ρ^+ production. This fact is a consequence of the large proton helicity flip amplitude in the latter case. It provides a substantial contribution to the cross section growing $\propto t'$, see Eq. (2). Therefore, the t dependence of $A_{UT}(\rho^+)$ is not approximately given by the factor $\sqrt{-t'}/2m$ as for the other vector mesons. In Fig. 5 we also show the t -integrated A_{UT} at $W = 10$ GeV, again evaluated from variant 1. The observed energy dependence is understandable considering the Regge behaviour of the various GPDs at low ξ .

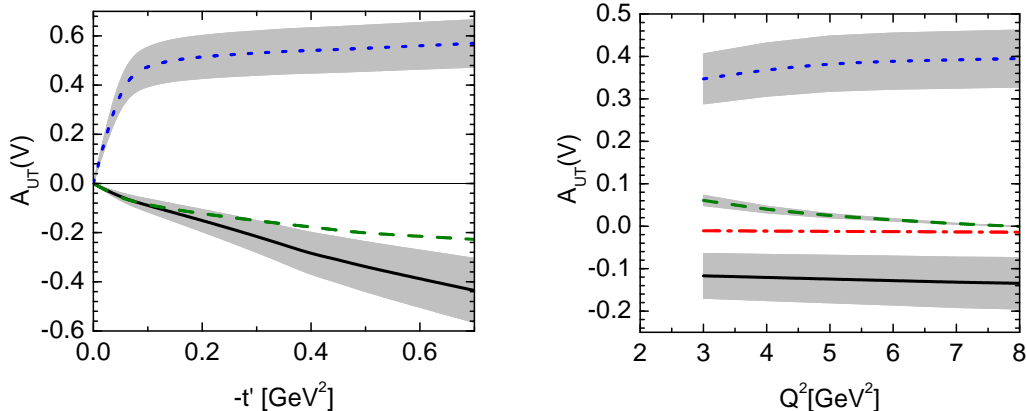


Figure 5: The asymmetry A_{UT} for various vector mesons versus t' at $W = 5$ GeV and $Q^2 = 3$ GeV² (left) and versus Q^2 at $W = 10$ GeV integrated upon t' (right), evaluated from variant 1. For notations refer to Fig. 1.

Before closing this section a few comments are in order. Frequently it is assumed that calculations to leading-twist accuracy of ratios like A_{UT} (see for instance [16, 19, 35]) might provide realistic estimates despite possible failures with the normalizations of the cross sections. This supposition relies on the assumption of a common K -factor for all amplitudes. In the modified perturbative approach which we are employing in the calculation of the subprocess amplitudes, this is however not the case with the exception of ρ^0 and ϕ production (see [6]). The most extreme example is ω production for which the leading-twist result is about a factor of 2 larger in absolute value than our result shown in Fig. 3.

COMPASS is using a transversally polarized deuteron target for electro-production of flavor-neutral vector mesons. Suppose the kinematics is chosen in such a way that the incoherent sum of proton and neutron scattering is essentially measured⁹. In this situation and regarding that, at $W \simeq 10$ GeV, the unpolarized cross sections for a proton and neutron target are about equal (the gluonic contribution dominates, see [2]) one has

$$A_{UT}(V^0 d) \simeq \frac{1}{2}[A_{UT}(V^0 p) + A_{UT}(V^0 n)], \quad (38)$$

for $V^0 = \rho^0, \omega, \phi$. Since the GPD E is dominated by valence quarks with $E_{\text{val}}^u \simeq -E_{\text{val}}^d$ as we repeatedly mentioned, one can readily see that $A_{UT}(V^0 d)$

⁹This may require large Q^2 , see for instance [36].

is approximately zero. This result is in agreement with preliminary COMPASS data on ρ^0 production [37]. The treatment of coherent scattering is beyond the scope of the present article.

Recently the SDME formalism has been developed [38] for the case of a proton target polarized perpendicular with respect to the hadron plane. These SDMEs are denoted by $n_{\mu\mu'}^{\sigma\sigma'}$ and related to bilinear combinations of the amplitudes for helicities μ, μ' and σ, σ' of the virtual photon and the meson, respectively. Taking into account the amplitudes (2) only the SDMEs n_{00}^{00} , n_{++}^{++} and n_{0+}^{0+} are non-zero. The first two are just A_{UT} for longitudinally and transversally polarized virtual photons, respectively. Their sum $n_{++}^{++} + \varepsilon n_{00}^{00}$ is the unseparated target asymmetry that we discussed above in great detail. These two SDMEs do therefore not provide any new information in contrast to n_{0+}^{0+} which is defined by

$$n_{0+}^{0+} = -(n_{+0}^{+0})^* = \frac{2}{N_T + \varepsilon N_L} \left[\mathcal{M}_{0-,0+}^N \mathcal{M}_{++,++}^{N*} - \mathcal{M}_{0+,0+}^N \mathcal{M}_{+-,++}^{N*} \right], \quad (39)$$

and for which we show results for ω and K^{*0} production in Fig. 4. Results for ρ^0 production can be found in [6].

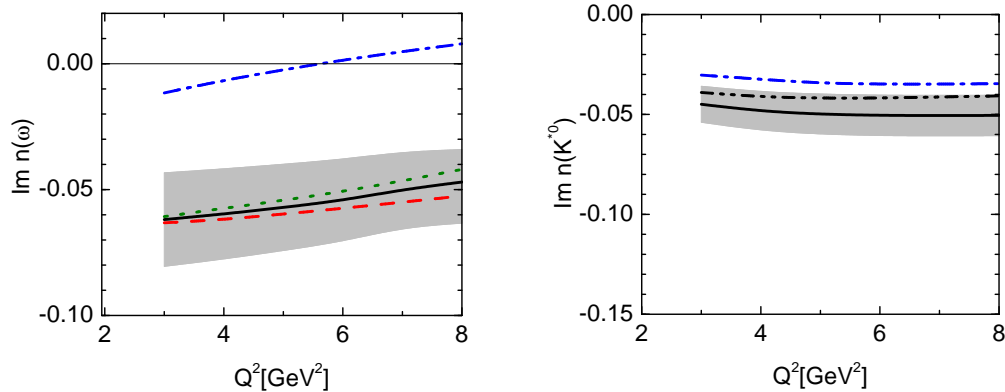


Figure 6: left: Left: The SDME $\text{Im } n_{0+}^{0+}$, integrated upon t , for ω (left) and K^{*0} (right) production versus Q^2 at $W = 5$ GeV. For notations refer to Figs. 2 and 4.

5 Concluding remarks

In this study we have investigated the target asymmetry for electroproduction of various vector mesons within the handbag approach. The hard subprocess amplitudes have been calculated employing the modified perturbative approach in which quark transverse degrees of freedom and Sudakov suppressions are taken into account. The GPDs are constructed from their forward limits combined with reggeized t dependences with the help of double distributions. The GPD H in particular has been modelled in our previous work [1, 2, 6] and shown to provide very good fits of the data on the longitudinal and transverse cross sections for ρ^0 and ϕ production in a large kinematical region. Here in this work we have taken H which controls the proton helicity-non-flip amplitude for small skewness, as given and have concentrated ourselves on the construction of E . This GPD builds up the proton helicity-flip amplitude required for the calculation of A_{UT} . As H it is constructed from double distributions and is constrained by the Pauli form factors of the nucleon, positivity bound and the sum rule (24). It turns out that for all variants we consider E is dominated by the valence quarks. This feature of E is to be contrasted with the behaviour of its counterpart H for which the gluons play the most prominent role for not too large momentum fractions.

The present experimental and theoretical knowledge does not allow to fix E uniquely. Therefore, we have considered a number of variants from which we have evaluated A_{UT} . It turns out that a particular pattern is obtained for it. The sign and size of A_{UT} is characteristic of the flavor nature of the respective vector meson. Hence, experimental data on A_{UT} for various vector mesons even if they are not very precise, may allow for a verification of the basic features of E like the prominent role of the valence quarks, and perhaps constrain its parameters tighter than it is actually the case. The present still preliminary data from HERMES, measured at rather small values of Q^2 , are fully consistent with our predictions. Since on the other hand they suffer from large errors they do not rule out any of the variants we presented, only the extreme variant 4 is slightly disfavored. Better data on A_{UT} for $Q^2 \gtrsim 3 \text{ GeV}^2$ are mandatory for a more accurate determination of E . Such data may be provided by HERMES and COMPASS and perhaps from experiments performed at the upgraded JLab (see [39]).

From the forward limits of H and E we have evaluated the angular momenta of the partons by means of Ji's sum rule. We have found for them a characteristic stable pattern which seems to be very hard to change drasti-

cally within the approach we advocated for. The spin of the proton is mainly built up by the u quarks and the gluons with only minor contributions from d and s ones. The connection between A_{UT} and the parton angular momenta seems to be quite general and does not strongly depend on a particular model for the GPDs which provide the link between these two quantities. Suppose the GPDs are smooth functions with no zeros except possibly at the endpoints. The convolution of the GPD with the propagators which build up the amplitudes should then show the same trend in size as the second moment of the GPD E , i.e. the contribution of E to Ji's sum rule. Moreover, with the exception of the ρ^0 case the t dependence of A_{UT} is dominated by the trivial factor $\sqrt{-t}/2m$ (see Eq. (2)) whose appearance is a consequence of angular momentum conservation. This implies that to a good approximation, A_{UT} provides information on E at $t \simeq 0$. In reality flavor decomposition of E matters and renders the analysis more difficult.

Acknowledgements

We thank A. Borissov, W.-D. Nowak, A. Sandacz and W. Vogelsang for discussions. We are also grateful to the HERMES collaboration for permission to use preliminary data. This work has been supported in part by the Heisenberg-Landau program and the Russian Foundation for Basic Research, grant 06-02-16215.

References

- [1] S. V. Goloskokov and P. Kroll, Eur. Phys. J. C **42**, 281 (2005) [hep-ph/0501242].
- [2] S. V. Goloskokov and P. Kroll, Eur. Phys. J. C **50**, 829 (2007) [hep-ph/0611290].
- [3] A. Rostomyan and J. Dreschler [HERMES collaboration], arXiv:0707.2486[hep-ex].
- [4] X. D. Ji, Phys. Rev. Lett. **78**, 610 (1997) [hep-ph/9603249].

- [5] F. Ellinghaus, W.-D. Nowak, A. V. Vinnikov and Z. Ye, Eur. Phys. J. C **46**, 729 (2006) [hep-ph/0506264].
- [6] S. V. Goloskokov and P. Kroll, Eur. Phys. J. C **53**, 367 (2008) [arXiv:0708.3569 [hep-ph]].
- [7] J. Botts and G. Sterman, Nucl. Phys. B **325**, 62 (1989).
- [8] L. Mankiewicz and G. Piller, Phys. Rev. D **61**, 074013 (2000) [hep-ph/9905287];
- [9] I. V. Anikin and O. V. Teryaev, Phys. Lett. B **554**, 51 (2003) [hep-ph/0211028].
- [10] L. L. Frankfurt, P. V. Pobylitsa, M. V. Polyakov and M. Strikman, Phys. Rev. D **60**, 014010 (1999) [hep-ph/9901429].
- [11] P. Ball and V. M. Braun, Phys. Rev. D **54**, 2182 (1996) [hep-ph/9602323].
- [12] P. Ball, V. M. Braun and A. Lenz, JHEP **0708**, 090 (2007) [arXiv:0707.1201 [hep-ph]].
- [13] M. A. Shifman and M. I. Vysotsky, Nucl. Phys. B **186**, 475 (1981).
- [14] M. Diehl, Phys. Rept. **388**, 41 (2003) [hep-ph/0307382].
- [15] M. Diehl and S. Sapeta, Eur. Phys. J. C **41**, 515 (2005) [hep-ph/0503023].
- [16] M. Diehl and W. Kugler, Eur. Phys. J. C **52**, 933 (2007) [arXiv:0708.1121 [hep-ph]].
- [17] M. Diehl, T. Feldmann, R. Jakob and P. Kroll, Eur. Phys. J. C **39**, 1 (2005) [hep-ph/0408173].
- [18] I. V. Musatov and A. V. Radyushkin, Phys. Rev. D **61**, 074027 (2000) [hep-ph/9905376].
- [19] J. Ossmann, M. V. Polyakov, P. Schweitzer, D. Urbano and K. Goeke, Phys. Rev. D **71**, 034011 (2005) [hep-ph/0411172].

- [20] X. D. Ji, J. Tang and P. Hoodbhoy, Phys. Rev. Lett. **76**, 740 (1996) [hep-ph/9510304].
- [21] P. Pobylitsa, Phys. Rev. D **66**, 094002 (2002) [hep-ph/0204337].
- [22] M. Burkardt, Phys. Lett. B **582**, 151 (2004) [hep-ph/0309116].
- [23] A. Donnachie Phys. Lett. B **611**, 255 (2005) [hep-ph/0412085].
- [24] M. V. Polyakov and C. Weiss, Phys. Rev. D **60**, 114017 (1999) [hep-ph/9902451].
- [25] P. Liebing [HERMES Collaboration], AIP Conf. Proc. **915**, 331 (2007).
- [26] CM. Alekseev *et al.* [COMPASS Collaboration], arXiv:0802.3023 [hep-ex]; E. S. Ageev *et al.* [COMPASS Collaboration], Phys. Lett. B **633**, 25 (2006) [hep-ex/0511028].
- [27] J. Pumplin, D. R. Stump, J. Huston, H. L. Lai, P. Nadolsky and W. K. Tung, JHEP **0207**, 012 (2002) [hep-ph/0201195].
- [28] Ph. Hägler *et al.* [LHPC Collaborations], arXiv:0705.4295 [hep-lat].
- [29] I. Balitsky and X. D. Ji, Phys. Rev. Lett. **79**, 1225 (1997) [hep-ph/9702277].
- [30] V. Barone, T. Calarco and A. Drago, Phys. Lett. B **431**, 405 (1998) [hep-ph/9801281].
- [31] J. Blümlein and H. Böttcher, Nucl. Phys. B **636**, 225 (2002) [hep-ph/0203155]
- [32] D. de Florian, R. Sassot, M. Stratmann and W. Vogelsang, arXiv:0804.0422 [hep-ph].
- [33] D. Yu. Ivanov, Proc. EDS07, Hamburg (2007).
- [34] W. Augustiniak [HERMES collaboration], talk presented at DIS08, London (2008).
- [35] K. Goeke, M. V. Polyakov and M. Vanderhaeghen, Prog. Part. Nucl. Phys. **47**, 401 (2001) [hep-ph/0106012].

- [36] J. Ashman *et al.* [EMC collaboration], *Z. Phys. C* **39**, 169 (1988).
- [37] A. Sandacz, talk presented at the workshop on 'Electromagnetic Interactions with Nucleons and Nuclei', Milos (2007).
- [38] M. Diehl, *JHEP* **0709**, 064 (2007) [arXiv:0704.1565[hep-ph]].
- [39] M. Strikman and C. Weiss, arXiv:0804.0456 [hep-ph].